J Appl Electrochem (2011) 41:543–550
DOI 10.1007/s10800-011-0264-5

ORIGINAL PAPER

Impact of electrode separator on performance of a zinc/alkaline/manganese dioxide packed-bed electrode flow battery

Bryan D. Sawyer · Galen J. Suppes · Michael J. Gordon · Michael G. Heidlage

Received: 22 October 2010 / Accepted: 10 February 2011 / Published online: 24 February 2011

Abstract A zinc/alkaline/manganese dioxide packed-bed electrode flow battery was used to evaluate using granular materials with ionic activity as separating materials between electrodes, increasing the separation distance between electrodes, while using separating materials, and reversing the electrolyte flow direction through the flow battery. Results indicate that materials with more ionic activity (ion exchange resins) perform better than materials with limited ionic activity (stainless steel). Among the more ionically active materials, the basic material out-performed the acidic material with an anode-to-cathode flow regime at low current draw. The best performance was obtained using ALL-CRAFT 4K-activated carbon as separation material. The use of an ionically active separation material reduced the difference in cell performance between 2.22 and 5.40 cm of separation by 56%. Although expected to be an important parameter for packed-bed electrode flow battery, the electrolyte flow direction did not produce a discernable difference in performance using the low current draw of these studies.

Keywords Battery · Flow · Energy · Packed-bed electrode · Electrolyte · Separator

1 Introduction

As more of the world progresses away from the complete use of liquid fossil fuel and advances toward the use of plug-in hybrid electric vehicle (PHEV) technologies for transportation use, there will be a high demand for larger scale, higher energy density electrical energy storage devices. These large-scale devices will also play a vital role in the sustainability of a renewable energy power grid by serving as point-of-source storage for excess electricity produced during off-peak periods. At times of peak electricity usage, the large storage devices will provide supplemental power to the power grid. The large-scale electrical energy storage devices will also benefit the renewable energy power grid by being able to efficiently store renewable electricity during intermittent times of high renewable electricity production by wind turbines and photovoltaic devices.

Current state-of-the-art battery systems, such as lithium-ion technology, are relatively expensive and have just recently been implemented for transportation use. Lithium-ion batteries use a specialized polymer separator to prevent electrical contact between the anode and cathode while still allowing for lithium-ion diffusion between the electrodes. The design and optimization of these separating materials is a science of its own and is continuously pursued by the battery industry to produce more efficient and safer batteries. The time and engineering applied to these separators lead to increased battery costs.

Cathode intercalation materials of the lithium-ion battery are also expensive. These materials are designed for reversible lithium-ion insertion (without reduction of the lithium ion) into the voids of their crystal structure. The cost of these cathode intercalation materials ranges depending on the metal being used in the material. Again, the time and engineering required for the optimization and development of these cathode intercalation materials drives up the cost of the final lithium-ion battery.

All conventional battery systems rely on bulk diffusion of ions between the anode and the cathode for operation.

B. D. Sawyer · G. J. Suppes (✉) · M. J. Gordon · M. G. Heidlage
Department of Chemical Engineering, University of Missouri, Columbia, MO 65211, USA
e-mail: suppesg@missouri.edu

Years of development have led to battery designs with very thin layers of active materials at each electrode separated by very thin separators to minimize diffusion distances, which have a positive impact on battery performance. The manufacturing of thin electrodes with thin layers of active materials coated on thin metal current collectors requires precision. The equipment and processing required for thin coating production lead to increased manufacturing costs, which ultimately increase final battery costs.

The costs associated with conventional diffusion-based battery technologies are acceptable for use in everyday items such as cell phones, laptop computers, and digital music players, but when the energy requirements are several magnitudes larger these costs can be problematic. A new design for large-scale electrical energy storage devices is needed to reduce total costs to make extreme scale-up economically feasible.

A new battery design will need to meet a long list of criteria to prove itself eligible for worldwide deployment. Such important criteria are high energy density, long cycle life, scalability (above a minimum threshold scale), high material utilization efficiency, deep cycle ability, applicability to various electrochemistries, and improved safety. It is also very important for the new battery design to be dominated by the cost of the electrochemically active components as opposed to highly engineered battery structure components.

In previous work, a validation of a packed-bed electrode zinc/alkaline/manganese dioxide battery with flowing electrolyte was discussed [1]. It was determined that increasing the separation between the anode and cathode had a negative impact on the cell potential, electrolyte flow had a positive impact on the cell potential, and that the presence of a strongly basic ion exchange resin between the anode and cathode had a positive impact on the cell potential. Based on these previous results, the goal of this work was to explore the use of other materials between the anode and cathode, impact of electrode separation distance in the presence of the materials between electrodes, and the impact of electrolyte flow direction (anode-to-cathode, cathode-to-anode) in the presence of the materials between electrodes. This work is applied to the zinc/alkaline/manganese dioxide battery chemistry, but it is important to understand that this design can be employed to other electrochemistries.

2 Background

The term "flow battery" [2–5] typically refers to electrochemical cells in which at least one of the active materials exists in a mobile phase. The operation of the flow battery requires the mobile active phase to circulate through the flow battery. Circulation of a mobile phase has the advantage of removing heat from the flow battery and, in cases where at least one active material is in the mobile phase, higher power output can be obtained by increasing the flow rate. A major advantage of the flow battery architectures is that money is saved through the elimination or reduction in size of needed separation membranes. There has been an abundance of previous research on flow batteries. Different flow battery architectures have been applied to numerous electrochemistries that employ soluble lead [6–8], soluble copper [9], soluble zinc [5, 10], thionyl chloride (liquid) [11], chlorine gas [12], and oxygen gas [13] as active components.

A distinction of the flow battery of this work is that all active materials exist and remain in a solid state in the packed-bed electrodes. The circulation of the electrolyte allows for the transfer of ionic intermediates between the electrodes to allow for the electrochemical reactions to proceed. A major advantage of solid active materials is that the activities of the materials remain nearly constant throughout use whereas both concentration and voltages from soluble active materials decrease during use. Batteries employing solid active materials tend to have higher energy densities due to a more constant operating voltage and higher molar densities of pure solid active materials versus solvated active materials.

In the flow battery of this work (Fig. 1), a pump circulates electrolyte between stacked electrodes. The goal is to pump ions between the electrodes at mass transfer rates greater than is possible with diffusion alone. The distances between electrodes in this specific design can be increased from 2.2 cm to any practical length. In conventional battery designs, the electrodes are only separated by separator

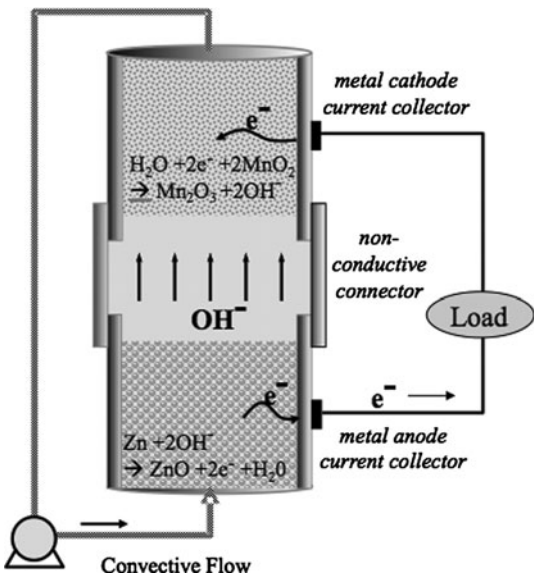

Fig. 1 Schematic of flow cell with packed bed electrodes

materials typically less than 50 μm thick. These short separation distances are easily traversed by dendrites that form when recharging metallic anodes and that is why most metallic anode batteries are not rechargeable. It is a benefit of the flow battery of this work to separate the electrodes by relatively large distances to eliminate the possibility of a dendrite induced short circuit, if in any case the dendrite formation cannot be controlled by the flow or control of flow of the electrolyte.

For small portable batteries the diffusion-based architectures are superior, as the cost of the circulating pump would cost more than the traditional diffusion-based battery. However, for larger batteries the savings in large areas of required separator can more than offset the cost of a pump. The higher active material to separating material (granular, not in sheet form) ratio of the packed-bed electrode flow battery makes it more economical for large-scale electrical energy storage needs. Typical applications of the packed-bed electrode flow battery would be plug-in hybrid electric vehicles and point-of-source electrical energy storage for load leveling applications.

This work is a discussion of the effects of using separation materials with different ionic behavior between the anode and cathode, the impact of separation distance in the presence of separation materials, and the effects of electrolyte flow direction on a packed-bed flow battery with all active materials in solid form.

3 Experimental

The packed-bed electrode flow cell used in these studies is shown in Fig. 2. It consists of a high-density polyethylene (HDPE) base fitted with a nylon hose barb to facilitate

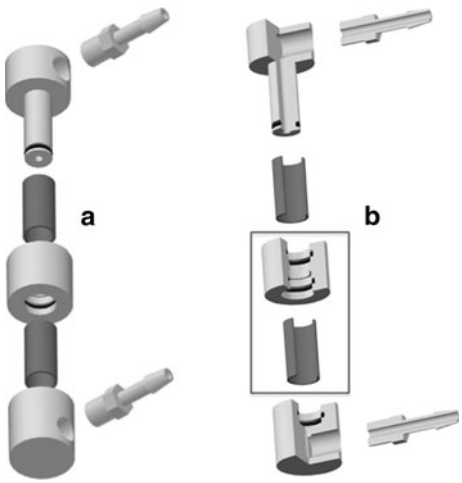

Fig. 2 **a** 3-D image of packed-bed electrode flow cell. **b** Cutaway of packed-bed electrode flow cell, parts in box are repeated to expand flow cell for use of granular separation material

electrolyte entry/exit, 1.27 cm outside diameter stainless steel tubes for anode and cathode current collection (also used for separation material section), HDPE separation couplings to maintain electrical isolation between the anode, cathode, and separation material sections, and a stainless steel piston (that slides into top electrode tube) top fitted with a nylon hose barb to facilitate electrolyte entry/exit. This piston top allows for compression to be applied to the packed electrode beds (using a small hydraulic press).

The flow cell was assembled from the bottom to the top. A single piece of Fisherbrand P8 filter paper punched into a circle with a 1.27 cm diameter was placed into the bottom the bottom HDPE piece to prevent material from being lost in the electrolyte entry/exit port. The anode collector tube was then inserted into the bottom HDPE piece by rotating and pressing it passed the o-ring seal, until it was seated tightly against the filter paper in the bottom of the HDPE bottom piece. Granular zinc (99.8%, 110–50 mesh, ACS reagent grade, Sigma-Aldrich) was then added into the anode current collector tube and hand packed until the zinc was level with the top of the anode collector tube. Then, a single piece of P8 filter paper punched to 1.27 cm in diameter was inserted into one side of a HDPE coupling until it rests evenly against the lip in the middle of the coupling. This side of the coupling containing the filter paper was then rotated and pressed over the end of the anode tube, until the anode tube was passed the o-ring seal and seated firmly against the filter paper and coupling lip. The separating material stainless steel tube was then pressed and rotated into the top of the HDPE coupling that was just attached to the anode, and separating material (separation materials were varied and will be detailed in specific subsections) was added and hand packed until the material was level with the top of the separating material tube. Like before, a piece of 1.27 cm diameter filter paper was inserted into the remaining HDPE coupling and the coupling was positioned onto the top of the separating material tube. The cathode current collection tube was then inserted into the top of the second HDPE coupling and the cathode material mixture consisting of 30 wt% manganese (IV) oxide (60–230 mesh, ≥99%, Sigma-Aldrich), 35 wt% graphite (Sigma-Aldrich), and 35 wt% 4K-activated carbon [14] was loaded and hand packed into the tube (the cathode tube is never filled completely because room is needed for the piston). Finally, the stainless steel piston (equipped with an o-ring seal) was inserted into the cathode current collection tube. Once fully assembled, the cell was placed in a small hydraulic press and enough pressure was applied to hold the cell in place, while electrolyte feed/discharge hoses are attached to the hose barbs of the cell. A two molar potassium hydroxide (≥90%, reagent grade, Sigma-Aldrich) solution (in distilled water) was used as the

electrolyte and was circulated through the flow cell using Masterflex Norprene peristaltic pump hose (Cole Parmer) and a Masterflex Easy Load II L/S pump head (Cole-Parmer) driven by a Masterflex console pump drive (Cole-Parmer). The electrolyte was pumped from a 60-mL reservoir and returned to the same reservoir upon exiting the flow cell for recirculation.

The flow cells were assembled as described above and were then connected to an external discharge circuit with switch automation for opening and closing the circuit. Voltage measurement and automated switch signals were provided by National Instruments LabVIEW software (using custom created virtual instrument files) through a National Instruments PCI-6229 data acquisition card connected to a National Instruments SCB-68 shielded connector block.

For all of the studies of this work, the flow cells were first subjected to a 45-min start-up period where electrolyte flow was initiated and allowed to reach a steady state. Near the end of this start-up period, the electrolyte flow rate through the flow cell was determined. Immediately following the start-up period, the flow cell was operated for 30-min open circuit period. After the open circuit period, the flow cell was discharged through a 550-Ω load for 30 min to obtain voltage profiles used in the analysis.

3.1 Survey of separating materials

Previous work indicated that the addition of an anionic ion exchange material into the tubular space between the anode and cathode increased the operating potential of the flow cell when compared to a stainless steel shot (0.4 mm, Pellets, LLC) control. In this study, a survey of materials with varying ionic properties were evaluated as separating materials between the anode and the cathode to determine effects on the operating cell potential. A 2.54-cm long stainless steel tube was used as a tubular separator between the anode and cathode and was filled with separating materials to be studied. The anode and cathode materials used are discussed above and the separating materials evaluated were Amberlyst A-26(OH) strongly basic ion exchange resin (Sigma-Aldrich), Amberlite IR-120H (Sigma-Aldrich) strongly acidic ion exchange resin, ethylene–acrylic acid copolymer beads (Allied-Signal, Inc.), stainless steel shot (0.4 mm, Pellets, LLC), and ALL-CRAFT 4K-activated carbon [14].

3.2 Impact of separation distance in presence of separation materials

It was determined in previous work that separation distance (in absence of separation materials) between the anode and cathode strongly affected the cell potential. It was determined that greater separation distances resulted in increasingly negative impacts on flow cell potential. This study is to determine the effects of electrode separation distance in the presence of separation materials.

The anode and cathode materials were the same as discussed above and only two separation materials were chosen for use in this study; Amberlyst A-26(OH) strongly basic ion exchange resin and stainless steel shot. The lengths of the middle separation tubes were varied to provide separation distances of 2.22, 2.86, 4.13, and 5.40 cm between the anode and cathode.

3.3 Impact of electrolyte flow direction

The operation of a zinc-alkali cell relies on the transportation of hydroxide ions between the anode and cathode. Hydroxide ions are consumed at the anode during discharge as shown in the half-cell reaction of Eq. 1. Hydroxide ions are produced in the cathode during discharge as shown in Eq. 2.

$$Zn + 2OH^- \rightleftarrows ZnO + H_2O + 2e^- \quad (1)$$

$$2MnO_2 + H_2O + 2e^- \rightleftarrows Mn_2O_3 + 2OH^- \quad (2)$$

The electrolyte flow was directed from anode-to-cathode and then from cathode to anode using both the Amberlyst A-26(OH) strongly basic ion exchange resin and the Amberlite IR-120H strongly acidic ion exchange resin as separation materials in a 2.54 cm long stainless steel middle section of tubing. Based on the electrochemistry, it is hypothesized that electrolyte flow direction will have an impact on the operating potential of the flow cell due to either having an excess or insufficient amount of hydroxide ions between the electrodes. Figure 3 provides a visual representation of the ion imbalance associated with a change in flow direction.

4 Results and discussion

4.1 Survey of separating materials

Figure 4 shows the impact of using materials with different ionic activity as the separating material between the anode and cathode. Initially, an 80 mV increase in operating potential, after a 30 min discharge through a 550-Ω load, was attributed to using Amberlyst A-26(OH) strongly basic ion exchange resin as the separating material in comparison with using stainless steel shot. Stainless steel was assumed to have very little ionic activity as it is designed to be a corrosion resistant material. Ethylene–acrylic acid copolymer beads were also assumed to have negligible ionic activity with the electrolyte and indeed the cell performance

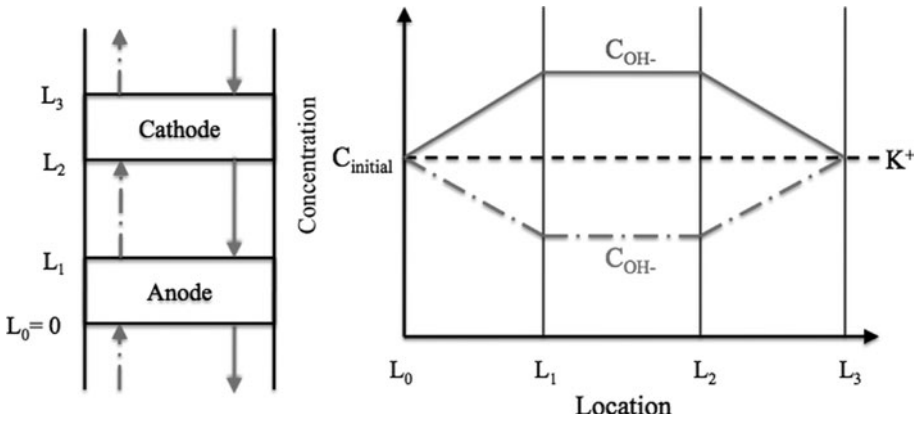

Fig. 3 Electrolyte flow direction impact on electrolyte ion concentration profile, *dash-dot line* correspond to anode-to-cathode flow and *solid line* corresponds to cathode-to-anode flow

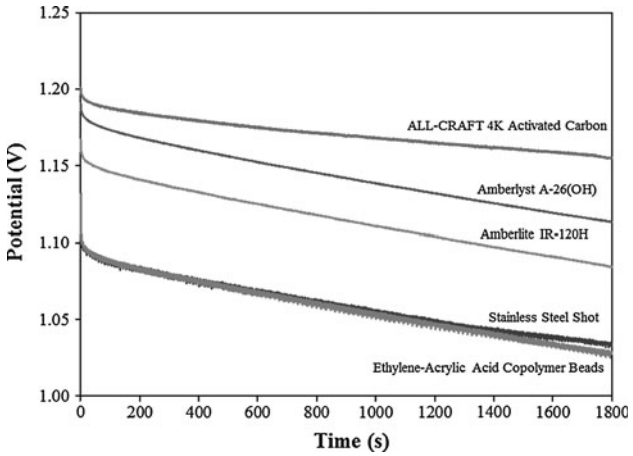

Fig. 4 Average voltage profiles for packed-bed electrode flow cell with varied separation material

using copolymer beads was very similar to the flow cell performance using stainless steel shot. This similarity can be seen in Fig. 4.

The voltage profiles shown in Fig. 4 were recorded as the electrolyte was circulated from the anode to the cathode. With OH^- ions being consumed in the anodic reaction (Eq. 1), there is a slight deficiency of OH^- ions in the separating section between the anode and cathode (See Fig. 3). It is believed that the strongly basic Amberlyst A-26(OH) helped to overcome the deficiency of OH^- present in the electrolyte and provided stability to the electrolyte flowing through the separating section between the electrodes. With the anionic exchange ions (OH^-) of the Amberlyst A-26(OH) resin being identical to those anions in the electrolyte, the exchange of ions will not affect the flow cell performance by altering the electrolyte.

Using the same anode-to-cathode flow regime, it was hypothesized that using a strongly acidic ion exchange resin in the separating section between the electrodes would have a negative impact on flow cell performance. A strong acidic cation exchange resin, such as Amberlite IR-120H, would provide a reservoir of cations (H^+) in the separating section where the electrolyte already contains an excess of cations (K^+) due to a deficiency of OH^- ions and would not help with flow cell performance. There would be an exchange of H^+ ions from the Amberlite IR-120H resin with the K^+ ions from the electrolyte. The H^+ ions migrating into solution will react with the OH^- ions present to produce water. Water formation consumes OH^- ions; preventing them from participating in the electrochemical reactions and dilutes the electrolyte. The electrolyte concentration is important because it is the driving force for the boundary layer diffusion of OH^- ions to the surface of solid active materials. It is important to note that the electrolyte solution would not be continually stripped of OH^- ions as to render it completely void of them because the interaction of the strongly acidic cation exchange material and the basic electrolyte solution would be constrained by equilibrium [15].

As seen in Fig. 4, the flow cell performance obtained using the strongly acidic Amberlite IR-120H ion exchange resin as separating material was better than using stainless steel shot but not as good as using the strongly basic Amberlyst A-26(OH). It was thought that the parasitic nature of the strongly acidic resin on the basic electrolyte would result in flow cell performance worse than that obtained using a neutral stainless steel shot. This was most likely due to minimal electrolyte degradation due to favorable equilibrium conditions between the Amberlite IR-120H and the potassium hydroxide electrolyte.

Based on the results of using acidic and basic ion exchange resins as separating materials in the flow cell it was decided to examine the use of an ALL-CRAFT-activated carbon as the separating material in the flow cell. Activated carbons are known to contain both acidic and basic reactive sites [16, 17]. Activated carbons are used as catalyst supports in packed-bed reactors and thus were not expected to pose a problem when used inside of the packed-bed flow cell.

It can be seen in Fig. 4, the use of ALL-CRAFT 4K-activated carbon as the separating material averaged a 40 mV increase in operating cell potential over the use of Amberlyst A-26(OH) at the end of a 30-min discharge through a 550-Ω resistive load. ALL-CRAFT-activated carbons are chemically activated using potassium hydroxide as the activating agent. Although the carbons are washed thoroughly after activation it is possible that the activation with potassium hydroxide imparts basic sites in the carbon's surface structure.

It has already been determined that a basic material exhibits better performance than an acidic material when used as a separating material in the flow cell. There could be a few reasons for the improved performance of the ALL-CRAFT 4K-activated carbon over the Amberlyst A-26(OH) ion exchange resin. The manufacturing steps of the 4K-activated carbon could provide stronger basic sites than those of the Amberlyst A-26(OH). Also, if the basicity of the materials is similar, then it could be the increased specific surface area of the smaller particle 4K-activated carbon that allows for better base site utilization and thus better performance.

An estimation of the particle size of the 4K-activated carbon was determined by passing the material through a set of sieves. Amberlyst A-26(OH) particles were then crushed using a mortar and pestle until visual comparison revealed particles similar in size to the 4K-activated carbon. The crushed Amberlyst A-26(OH) and 4K-activated carbon were collected from the same sieve trays for use in this study. The size range of these materials was 180–400μm, and the size range of the stock Amberlyst A-26(OH) was 400–595 μm. A comparison of the flow cell performance between the ALL-CRAFT 4K-activated carbon, stock Amberlyst A-26(OH), and reduced particle size Amberlyst A-26(OH) is shown in Fig. 5. The ALL-CRAFT 4K-activated carbon performed better and the similar sized small particle Amberlyst A-26(OH) performed worse than the stock Amberlyst A-26(OH), so particle size can be ruled out as a reason for the performance gain of the 4K-activated carbon.

The flow cell performance results shown in Figs. 4 and 5 suggest that the ALL-CRAFT 4K-activated carbon benefits flow cell performance by exhibiting a higher basicity than the Amberlyst A-26(OH). The basicity maybe inherent in the material structure or it could be a product of electrolyte uptake into the pores of the activated carbon by way of absorption that acts as an electrolyte reservoir. This work does not determine by what mechanism the activated carbon provides better flow cell performance, only that it does provide better performance by providing increased basicity.

4.2 Impact of separation distance in presence of separation materials

In previous work, it was determined that, in the absence of a separating material, flow cell performance decreased with an increase in the separation distance between the anode and cathode [1]. It is ideal to operate the flow cell with a minimum of a few centimeters of separation between the anode and cathode to dramatically reduce the possibility of an internal short circuit failure. In an effort to compensate for the reduced performance at greater separation distances a look into flow cell performance at various separation distances in the presence of separation materials was conducted.

Figure 6 shows the performance of flow cells using Amberlyst A-26(OH) and stainless steel shot separation materials. Each material was evaluated in the flow cell with separation distances of 2.22, 2.86, 4.13, and 5.40 cm

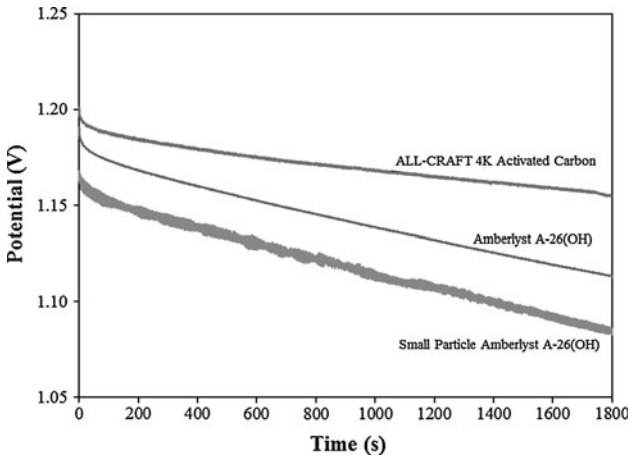

Fig. 5 Average voltage profiles for packed-bed electrode flow cell comparing similar particle size ALL-CRAFT 4K-activated carbon (180–400 μm) and small particle Amberlyst A-26(OH) (180–400 μm) to original Amberlyst A-26(OH) (400–595 μm)

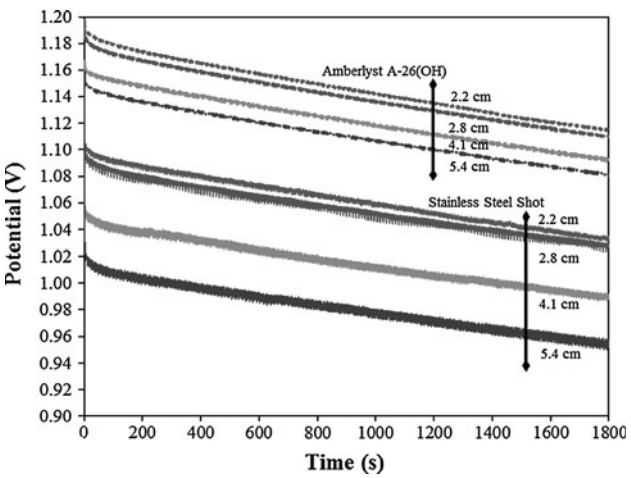

Fig. 6 Voltage profiles for packed-bed electrode flow cell using two different separation materials, each at four different separation distances

between the electrodes. Based on flow cell performance shown in Fig. 4, it was assumed that using stainless steel shot as the separation material would have lower performance than using the Amberlyst A-26(OH) and this remained true. In keeping with the same separation material, there is still a reduction in flow cell performance at increasing separation distances, but it is important to note that the Amberlyst A-26(OH), exhibited a much tighter range in performance between separation distances of 2.22 and 5.40 cm. There is about a 35 mV range in final voltage measurements between 2.22 and 5.40 cm of separation using Amberlyst A-26(OH). This is a 56% reduction from the 80 mV range between 2.22 and 5.40 cm of separation using stainless steel shot. The major improvement in flow cell performance associated with using Amberlyst A-26(OH) at 5.40 cm of separation between electrodes as opposed to using stainless steel shot at only 2.22 cm of separation indicates that the use of separation materials that interact positively with the electrolyte allow the cell to be operated with sufficiently large separation distances with minimal performance loss compared to using a separation material that does not ionically interact with the electrolyte.

4.3 Impact of electrolyte flow direction

The impact of electrolyte flow direction on the flow cell was determined by circulating the electrolyte in an anode-to-cathode flow regime and then in a cathode-to-anode flow regime in the presence of both acidic (Amberlite IR-120H) and basic (Amberlyst A-26(OH)) ion exchange resins. It was hypothesized that the flow direction would have a dramatic impact on the flow cell performance because the electrolyte between the electrodes will have either an excess of OH^- ions or K^+ ions, and these ions will each interact with the separation material differently. It is believed than an acidic ion exchange resin used as a separating material would perform better than a basic ion exchange resin in the case of the electrolyte having excess OH^- ions due to charge balancing interactions between the electrolyte and separating resin. For the same reason, it is believed that use of a basic ion exchange resin as the separating material would perform better with electrolyte flowing from the anode to the cathode, as there would be an excess of K^+ ions in the solution.

The flow cell voltage profiles using both Amberlite IR-120H and Amberlyst A-26(OH) as separating materials with both electrolyte flow directions are shown in Fig. 7. The flow cell performance using Amberlite IR-120H for the separating material is represented by the lower group of voltage profiles, while the flow cell results using Amberlyst A-26(OH) are shown in the higher group of voltage profiles. The solid lines show flow cell results obtained with electrolyte flowing from the anode to the cathode, and the dotted lines are results obtained with electrolyte flowing from cathode to anode.

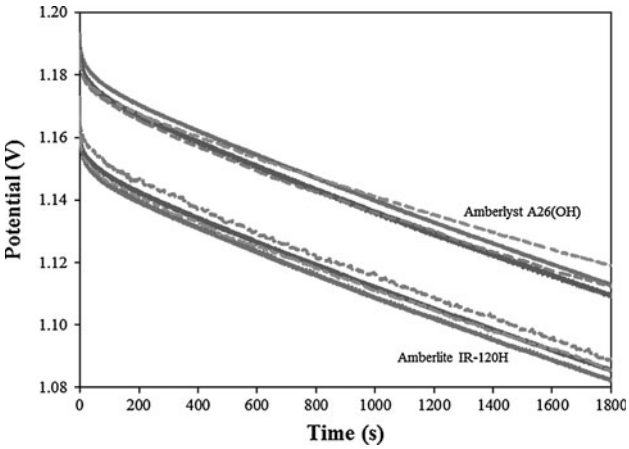

Fig. 7 Voltage profiles for packed-bed electrode flow cell using an acidic and basic ion exchange resin as separation material; *solid lines* were obtained with an anode-to-cathode flow regime and *dashed lines* were obtained with a cathode-to-anode flow regime

As shown in Fig. 7, the Amberlite IR-120H voltage profiles show only marginal performance gains associated with circulating the electrolyte from the cathode to the anode as opposed to anode-to-cathode circulation with a resistive load of 550-Ω applied to the flow cell. The excess OH^- ions in the electrolyte between the electrodes interact with the acidic Amberlite IR-120H, and this helps to stabilize the excess charge and provide better flow cell performance. It would be expected that increasing the discharge rate would result in a greater differences in flow cell performance associated with the two electrolyte flow directions. An increase in the discharge rate is analogous to either consuming (at anode) or producing (at cathode) more OH^-, thus creating a larger charge imbalance in the electrolyte between the electrodes.

Figure 7 also shows that there were also small performance gains associated with circulating electrolyte from the cathode to the anode (excess OH^- between electrodes) through the basic Amberlyst A-26(OH) resin. This is contrary to what was believed would happen, as with the basic resin it was hypothesized that an excess of K^+ ions between the electrodes would exhibit better flow cell performance. This contradiction indicates the possibility that discharging through 550-Ω may produce too slow of a discharge rate to determine a discernable difference in flow cell performance between the two different flow regimes and that the marginal improvement discussed above for the Amberlite IR-120H may not be large enough to be deemed significant. A faster discharge rate would make the ionic imbalance between the electrodes larger. The lack of complete dependence of performance on the direction of electrolyte flow may indicate a further dependency on electrolyte concentration and flow velocity.

5 Conclusions

A survey of materials used in the separating section between the electrodes of a packed-bed flow cell revealed that materials with basic properties outperform acidic and neutral materials. An interesting discovery was that an ALL-CRAFT 4K-activated outperformed the strongly basic Amberlyst A-26(OH) when used as separating material in the flow cell. Particle size was ruled out as a reason for the 4K-activated carbon success as similar size particles of 4K-activated carbon and Amberlyst A-26(OH) resulted in voltage profiles above and below the voltage profile of stock Amberlyst A-26(OH), respectively.

A previous study indicated that an increase in the separation distance between the electrodes reduced the flow cell voltage. The present evaluation demonstrated that certain separator materials substantially reduce the loss in voltage associated increasing separation distances.

Although expected to make a difference at higher discharge rates, electrolyte flow direction had minimal impact while discharging through a 550-Ω load. It is expected for high discharge rate applications that the electrolyte flow direction will be an important factor to obtain optimal flow cell performance.

Acknowledgment A special thanks is extended to the National Science Foundation (Award 0940720) for their generous financial support.

References

1. Suppes GJ, Sawyer BD, Gordon MJ (2010) High-energy density flow battery validation. AIChE J (in press). doi: 10.1002/aic.12390
2. Cheng J, Luo X, Yan X et al (2008) Sci Chin B 51:709
3. Radford GJ W, Cox J, Wills RGA et al (2008) J Power Sources 185:1499
4. Wang X, Wang Y, Xue F et al (2009) US Patent No 2008-20108417
5. Zhang L, Cheng J, Yang Y-S et al (2008) J Power Sources 179:381
6. Hazza A, Pletcher D, Wills R (2004) Phys Chem Chem Phys 6:1773
7. Li X, Pletcher D, Walsh FC (2009) Electrochim Acta 54:4688
8. Pletcher D, Wills R (2005) J Power Sources 149:96
9. Pan J, Sun Y, Cheng J et al (2008) Electrochem Commun 10:1226
10. Cheng J, Zhang L, Yang Y-S et al (2007) Electrochem Commun 9:2639
11. Puskar M, Harris P (1986) Proc. Int. Power Sources Symp. 32nd:331
12. Hart TG (1980) US Patent No 4237197
13. Pan J, Ji L, Sun Y et al (2009) Electrochem Commun 11:2191
14. Pfeifer P, Suppes GJ, Shah P et al (2008) World Patent No. 2008058231
15. De Lucas A, Zarca J, Canizares P (1992) Sept Sci Technol 27:823
16. Leon CA, Leon D, Radovic LR (1994) Chem Phys Carbon 24:213
17. Lopez-Ramon MV, Stoeckli F, Moreno-Castilla C et al (1999) Carbon 37:1215